Article

Discovery Medicine 2024; 36(187): 1572–1587
https://doi.org/10.24976/Discov.Med.202436187.144

Idebenone-Loaded Nanocomposite Microspheres for Nasal Administration—A Perspective in the Treatment of Alzheimer's Disease

Radka Boyuklieva[1,2], Plamen Katsarov[1,2], Plamen Zagorchev[2,3], Silviya Abarova[4], Asya Hristozova[5], Bissera Pilicheva[1,2,*]

[1]Department of Pharmaceutical Sciences, Faculty of Pharmacy, Medical University of Plovdiv, 4002 Plovdiv, Bulgaria
[2]Research Institute, Medical University of Plovdiv, 4002 Plovdiv, Bulgaria
[3]Department of Medical Physics and Biophysics, Faculty of Pharmacy, Medical University of Plovdiv, 4002 Plovdiv, Bulgaria
[4]Department of Medical Physics and Biophysics, Faculty of Medicine, Medical University of Sofia, 1000 Sofia, Bulgaria
[5]Department of Analytical Chemistry and Computational Chemistry, Faculty of Chemistry, University of Plovdiv "Paisii Hilendarski", 4000 Plovdiv, Bulgaria
*Correspondence: bisera.pilicheva@mu-plovdiv.bg (Bissera Pilicheva)
Published: 20 August 2024

Background: Alzheimer's disease results in neurodegeneration and is characterized by an accumulation of abnormal neuritic lesions and intracellular aggregates of hyperphosphorylated Tau proteins in the cerebrum. That leads to progressive decline in memory, thinking, and learning skills. Oxidative stress has been shown to play a significant role in the pathogenesis of Alzheimer's disease. Antioxidants are identified as part of therapeutic strategy to prevent or reduce the disease. Idebenone is a synthetic analogue of coenzyme Q_{10} with potent antioxidant properties, originally developed for the treatment of Alzheimer's disease and other cognitive disorders. After oral administration idebenone undergoes excessive first-pass metabolism and has a very low bioavailability of only about 1%. The use of an alternative route of administration such as the nasal and its incorporation into a novel carrier (nanocomposite microspheres) will eliminate the problems associated with reduced absorption, stability, and rapid biotransformation and will increase the opportunity for idebenone to realize its therapeutic potential in Alzheimer's disease.
Methods: Idebenone-loaded nanocomposite microspheres were obtained by spray drying. The structures were characterized using laser diffraction, scanning electron microscopy, high-performance liquid chromatography, Fourier-transform infrared spectroscopy, and differential scanning calorimetry. The ability of nanocomposite microspheres to bind human serum albumin was investigated by fluorescence spectroscopy. The mucoadhesive properties of the carrier were also determined.
Results: Bioadhesive nanocomposite microparticles with spherical shape, smooth surface, size of 7.37 $\pm$ 2.4 µm, and with high production yield, good drug entrapment efficiency, and loading values were obtained. Infrared spectra demonstrated no chemical interactions between idebenone and structure-forming polymers. The ability of particles to bind to human serum albumin depends on their drug loading.
Conclusions: Nanocomposite microspheres were developed as the novel delivery system of idebenone for target nose-to-brain delivery. The obtained carrier may increase the therapeutic potential of idebenone by providing higher concentrations in brain tissue and reducing systemic exposure and side effects.

Keywords: idebenone; nanocomposite microspheres; nose-to-brain delivery; Alzheimer's disease

Introduction

Alzheimer's disease (AD) is a multifactorial condition resulting from genetic, epigenetic, and environmental risk factors [1]. It affects more than 38 million people worldwide and manifests clinically with memory, cognitive and behavioural impairments that result in permanent disability and inability to cope with daily needs. Due to the aging of the population, a noticeable rise in the number of affected subjects is predicted—about 152 million by 2050 [2]. Elevated levels of neurotoxic proteins such as Aβ and Tau are major diagnostic criteria. Their synthesis is initiated and increased mainly by redox imbalance arising as a consequence of a disparity between antioxidants and free radicals [3]. Free radicals are atoms, groups of atoms, or molecules that contain one or more unpaired electrons in their outer shell. The brain is rich in biometals and lipids susceptible to oxidation and has an increased need for oxygen. When molecular oxygen is reduced, powerful free radicals are generated. Initially, a superoxide radical ($O_2^{\bullet -}$) is formed, which produces hydrogen peroxide (H_2O_2) by the addition of an electron. *In vivo*, $O_2^{\bullet -}$ is formed in mitochondria un-

der the control of enzymatic and non-enzymatic processes. Reduction of H_2O_2 leads to the production of highly reactive hydroxyl radicals (OH•) called reactive oxygen species (ROS). Under normal conditions, neurons are able to neutralize the generated free radicals. This is accomplished in the mitochondria by various enzyme systems such as superoxide dismutase, cytochrome c and glutathione peroxidase [4]. Ubiquinol (QH2), another electron carrier with a detoxifying function, reduces various peroxides in the presence of succinate. With increasing age, the ability of cells to reduce free radical damage declines. Also, the brain has lower antioxidant activity than other organs (about 10% of that of the liver) [5]. The excessive production of $O_2^{\bullet -}$ and H_2O_2 in the presence of catalytic Fe and Cu ions, highly reactive OH• radicals and other pro-oxidant molecules are formed. They have high reactivity and rapidly bind to cellular proteins, lipids, and nucleic acids thereby changing their structure and functions. The oxidative stress results in apoptosis—the programmed destruction of cells once they become dangerous to the organism in which they develop. However, the structurally altered proteins and lipids are not degraded, but remain in the brain tissue and interfere with its normal functioning.

Although an optimal treatment of AD is still lacking, research activities are aimed at (i) increasing the effectiveness of current drugs by incorporating them in convenient dosage forms and (ii) exploring new routes of administration, invasive (intravenous and intracranial) or alternative (non-invasive, e.g., nasal administration) [6]. Modern therapy includes medications administered orally in the form of tablets and capsules. Available drugs do not lead to permanent improvement/complete cure of the disease and have a number of disadvantages. One of them is the low bioavailability of drugs in the central nervous system (CNS) after systemic administration.

Antioxidant therapy has been investigated for years as one of the prospective therapies for the prevention and treatment of neurodegenerative diseases. It is well known that the imbalance of free radicals and antioxidants over a long period of time damages the structure and functions of the cellular respiratory apparatus, the mitochondria, throughout the progression of AD [7]. Therefore, the various mitochondria-protecting agents refer to metabolic antioxidants. Those antioxidants, including derivates of vitamin E and coenzyme Q10 (CoQ_{10}), which can enter not only the cell but also the mitochondria, thus protecting the cells to the greatest extent from oxidative stress. Idebenone (IDB) is a synthetic analogue of CoQ_{10}, a short-chain benzoquinone with potent antioxidant properties originally developed for the therapy of AD and other cognitive disorders. The active hydroquinone form of IDB is produced in cells after reduction by nicotinamide adenine dinucleotide phosphate (NADP)H-quinone oxidoreductase 1. After activation, IDB participates in electron transport in mitochondria and enhances adenosine triphosphate (ATP) synthesis. IDB protects cellular structures from the harmful effects of superoxide anion radicals, reduces lipids peroxidation, damage to cell structures, and prevents cell death. Subsequently, IDB has been investigated for the treatment of some uncommon diseases like Friedreich's ataxia, Leber's hereditary optic neuropathy, Duchenne muscular dystrophy, mitochondrial encephalopathy, lactic acidosis, and primary progressive multiple sclerosis [8,9]. Recently, it has been reported that under conditions of hypoxia, IDB prevents the release of mitochondrial DNA and the subsequent activation of the NLRP3 (nucleotide-binding domain, leucine-rich–containing family, pyrin domain–containing-3) inflammasome, thereby interfering with one of the earliest stages of the proinflammatory cascade. This suggests inflammatory CNS conditions may be treatable with IDB. Based on the findings on the molecular mechanism of action of IDB, new indications for its use are expected to be identified [10]. However, no significant improvement in cognitive function was observed in clinical trials on patients with Alzheimer's disease [11]. IDB is water-insoluble and rapidly absorbed taken orally in the form of tablets or capsules. Unfortunately, after oral administration IDB undergoes significant presystemic metabolism. Only about 1% of the initially taken dose reaches the systemic circulation unchanged. The incorporation of IDB into liquid dosage form, e.g., suspensions, and its intake of fat-rich foods increases its bioavailability in humans to a maximum of 14% [12]. In addition, most of the absorbed drug binds to plasma proteins, which also reduces its distribution and concentration in the brain, thus hindering its therapeutic potential. Some adverse effects of IDB after oral administration have also been reported, which may be due to the need for higher doses for beneficial neurological effects. Such adverse effects are stomach pain, diarrhoea, nausea and vomiting, tachycardia and increased risk of infections, nasopharyngitis, cough and back pain. The use of an alternative route of administration that will ensure targeted delivery of IDB to the CNS will reduce the dose and thus the systemic exposure to the drug and prevent side effects.

The brain is a highly sensitive neuronal organ protected by vascular barriers that regulate the entry of substances based on the needs of the CNS. Treatment of diseases affecting the CNS is hampered by the presence of physiological, metabolic, and biochemical barriers created by the blood-brain, blood-cerebrospinal fluid, and arachnoid barriers [13,14]. It has been shown that approximately 90% of low-molecular-weight drugs, including lipophilic compounds, and nearly 100% of proteins and nucleic acids used for therapy do not reach brain tissue because of barrier systems. To cross the blood-brain barrier, drug molecules must be nonionized with lipophilic structure, with a low molecular weight (below 500 Da), and with the ability to form no more than 8 hydrogen bonds [15]. The route of drug administration affects the distribution of active molecules in the brain. The gentle, harmless, inoffen-

sive routes for drug delivery to the CNS are oral, buccal, sublingual, rectal, and intranasal. Orally administered drugs may undergo intense hepatic metabolism before reaching the circulatory system. After sublingual, rectal, and buccal administration drugs enter the systemic circulation directly. They must cross the blood-brain barrier to reach the target brain tissue. The direct administration of active substances into the CNS is performed by intrathecal, intracerebro-ventricular or intraparenchymal injections, which are placed into the cerebrospinal fluid. Continuous drug delivery can be provided using implants [16]. Although in clinical use, the above techniques are invasive and their use is limited to hospital settings. Therefore, there is a need to develop a safe and efficient platform for the delivery of active molecules to the CNS. This determines the need to explore an alternative drug delivery route.

The research community has shown increasing interest in intranasal administration of drugs for direct delivery to the CNS (nose-to-brain, N2B) [17–19]. This possibility was unexplored until 1991, when William Frey III [20] patented a method of nasal drug delivery for the treatment of neurological diseases [20].

Intranasal administration provides rapid drug absorption due to the rich blood supply to the nasal mucosa and the high permeability of the epithelium. Drugs resorbed through the nasal mucosa can enter directly the systemic circulation or CNS, thus avoiding inactivation in the gastrointestinal tract. Nasal dosage forms are easily, non-invasively and painlessly administered, which meets with high patient approval [21].

Nasal dosage forms for direct N2B delivery are appropriate for active substances that have no therapeutic effect when administered orally, for an extended period of time, require small doses and rapid entry into the circulation. For example, dopamine administered orally cannot be used to treat Parkinson's disease because it is unable to pass through the blood-brain barrier. In a study of its levels in the blood and cerebrospinal fluid of rats, increased levels of dopamine were recorded in the brain 30 min after nasal administration, which was not observed after intravenous administration. The data suggest that dopamine is transported to the olfactory bulb in an unaltered state via the olfactory pathway [22]. Clinical trials have confirmed high levels in the brain of peptides such as melanocortin, vasopressin, and insulin after nasal administration. Therefore, these peptides positively affect cognitive functions [23]. Intranasal administration of insulin improves cognitive functions in AD patients without elevated peripheral blood levels [24]. Of key importance for the rate of diffusion of substances across the nasal mucosa, as with other biological membranes, are their physicochemical characteristics (molecular mass, lipophilicity, degree of dissociation) [25,26]. The nasal route also poses some challenges. One of the most serious obstacles to nasal absorption is the rapid removal of the administered dosage form due to enhanced mucociliary clearance in the nasal mucosa [25]. With reliable drug delivery systems, this can be avoided by delivering drug molecules to the target site.

Different strategies can be applied to increase the intracerebral concentration of IDB to achieve higher efficacy of CNS disorders therapy compared to common dosage forms. For example, intranasal application of IDB-loaded nanocarriers can deliver active molecules to brain tissue via transport across the olfactory and trigeminal nerves, bypassing systemic barriers and presystemic metabolism. This is possible due to the direct connection between the olfactory region and the brain. In addition, the transport of drugs from the olfactory region to the brain is considered effective in humans [25]. Thus, the treatment of degenerative CNS isorders such as AD may have a greater success. Nanoparticles can protect the drug from enzymatic and chemical degradation and facilitate its passage through membrane barriers. Despite the listed advantages, nanoparticles due to their small size when inhaled follow the respiratory tract and exit the nasal cavity. Whereas microparticles larger than 5 μm to about 10 μm in diameter are preferentially deposited in the olfactory region, but due to their larger size they cannot transport therapeutic agents directly to the brain [27–29]. Therefore researchers are expanding the scope of synthesis from basic structures, such as micro- and nanoparticles, to more complex carriers. Nanocomposite microparticles are a new variety of drug delivery systems that consist of nanosized particles dispersed in a polymer matrix [30]. By designing the composite structure, carriers with specific physicochemical and mechanical characteristics are obtained. These structures are a combination of the best properties of their components, while also exhibiting interesting characteristics that the individual ingredients often do not possess [31]. The development of nanocomposite microspheres with optimal bioadhesive and biopharmaceutical properties is a challenge for modern pharmaceutical technology. Successful implementation of which is a prerequisite for the creation of an innovative and easy-to-use drug carrier for nasal administration of active substances in the therapy of neurodegenerative diseases. This article focuses on the development of a drug delivery system with the potential for targeted delivery of IDB to the CNS.

Materials and Methods

Materials

Idebenone (IDB, Mw 338.44 g/mol, № I5659), poly-ε-caprolactone (PCL, Mw 14,000 g/mol, № 440752), sodium alginate (from brown algae, medium viscosity ≥2000 cP, 2% (25 °C), № A2033), Polysorbate 20 (№ P1379), Polysorbate 80 (№ P1754), 2,2-Diphenyl-1-picryl hydrazyl (DPPH, № D9132), human serum albumin (≥96%, № A1653) were purchased from Sigma-Aldrich (St. Louis, MO, USA). All other reagents and solvents were of analytical grade.

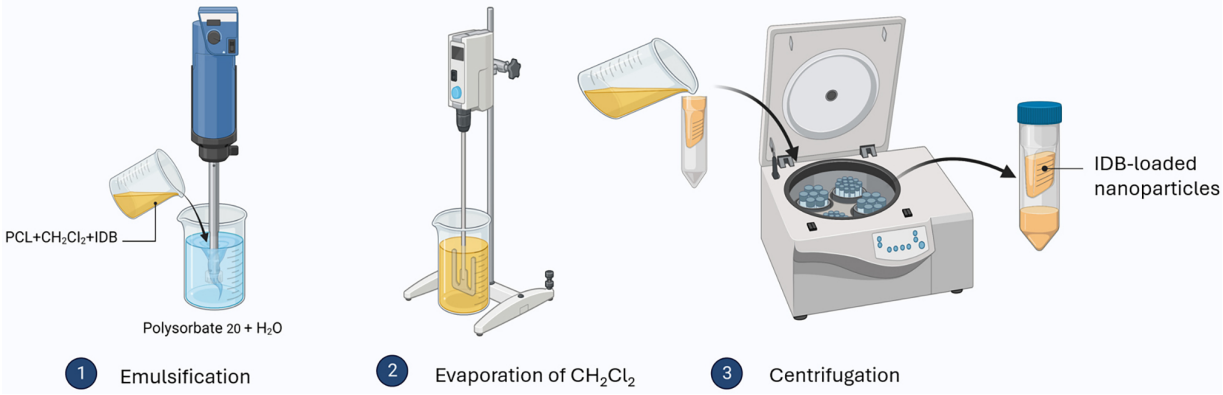

Fig. 1. Preparation of idebenone (IDB)-loaded nanoparticles by emulsion solvent evaporation method. (1) preparation of oil-in-water emulsion, (2) organic solvent evaporation, (3) separation of the nanoparticles. Created with BioRender (https://www.biorender.com).

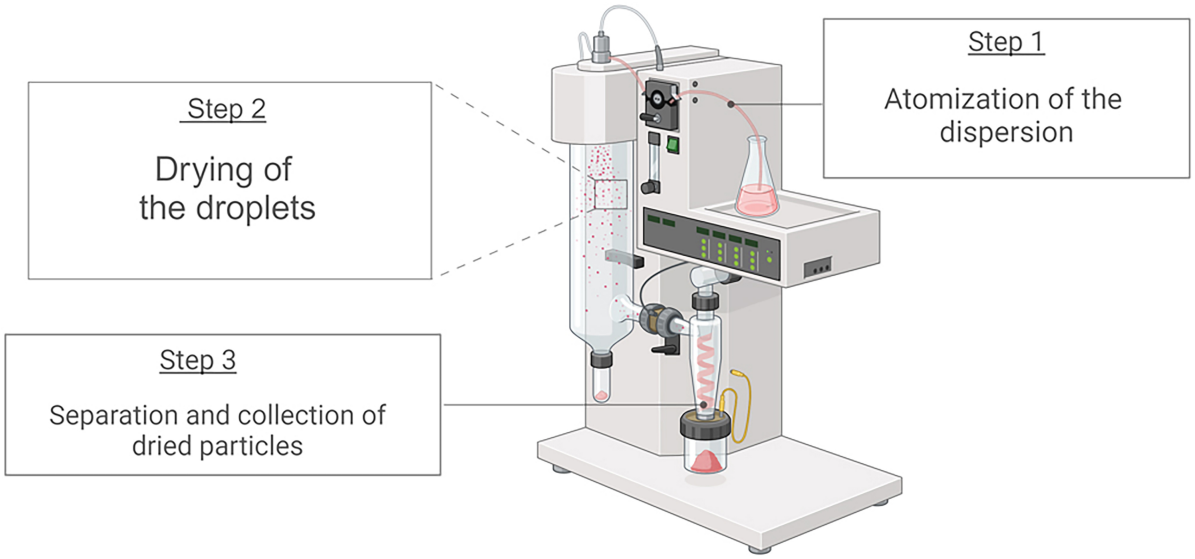

Fig. 2. Main steps in preparation of nanocomposite microspheres by spray drying. Created with BioRender (https://www.biorender.com).

Synthesis of IDB-Loaded Nanoparticles

IDB-loaded nanoparticles, composed of IDB and PCL in ratio 1:1.25, were obtained by emulsion/solvent evaporation method, as previously reported [32].

In brief, the drug and polymer were fully dissolved in dichloromethane. Due to the lipophilic nature of IDB, an oil-in-water (O/W) emulsion type was chosen to be prepared. First, O/W emulsion was formed as the solution of IDB and PCL was added to the water phase containing Polysorbate 20 as an emulsifier under high-speed homogenization at 25,000 rpm for 3 min. The obtained nanoemulsion was then stirred on an overhead stirrer at 800 rpm until complete evaporation of dichloromethane and solidification of the PCL droplets. The nanoparticles were separated by centrifugation of the suspension in Amicon® tubes (Merck KGaA, Darmstadt, Germany) at 3800 $\times g$ for 20 min at 20 $\pm$ 1 °C (Fig. 1).

Formulation of IDB-Loaded Nanocomposite Microspheres

PCL nanoparticles without drug (placebo) or loaded with IDB (quantity of nanocarriers equal to 200 mg IDB) were dispersed in an aqueous solution of sodium alginate (concentration 0.5% or 1% w/v, volume 100 mL). The obtained dispersions are taken to the spray dryer by means of a peristaltic pump at a speed of 6/9 mL/min with continuous stirring with an electromagnetic stirrer (500 rpm). The atomization is carried out through a nozzle with a diameter of 0.7 mm while varying the inlet temperature of the drying gas from 120 °C to 160 °C. Nitrogen under a pressure of 5 bar, supplied at a rate between 400/600 L/h, was used for atomization. To separate and collect the dry particles, the pulverization of the material was carried out at an aspiration of 35 m^3/h (Fig. 2).

Characterization Techniques

Particle Size Analysis and Size Distribution

The size of the nanocomposite microparticles and their size distribution were determined by laser diffraction with a LS 13 320 Particle Size Analyzer for dry and wet dispersions (Beckman Coulter, Brea, CA, USA) equipped with a Tornado Dry Powder System. One hundred milligrams of particles were used for each measurement (n = 3).

Scanning Electron Microscopy (SEM)

Visualization of the obtained particles was performed by scanning electron microscopy (Prisma E SEM, Thermo Scientific, Waltham, MA, USA). The samples were dried and then loaded on an aluminium stubs and sputter coated with gold using a vacuum evaporator (Q150T ES Plus, Quorum technologies, West Sussex, UK). The images were recorded at 15 kV acceleration voltage at 3500 magnifications using an Everhart–Thornley detector (ETD).

Fourier-Transform Infrared Spectroscopy (FTIR)

FTIR spectroscopy was used to investigate possible chemical interactions between the drug and the polymer. The spectra were collected in the range from 600 cm^{-1} to 4000 cm^{-1} with a resolution of 4 nm and 32 scans, using a Nicolet iS 10 FTIR spectrometer (Thermo Fisher Scientific, Pittsburgh, PA, USA). The instrument is equipped with a diamond attenuated total reflection (ATR) accessory and the spectra were analysed with the OMNIC® software package (Version 7.3, Thermo Electron Corporation, Madison, WI, USA).

Differential Scanning Calorimetry (DSC)

Thermal analysis of the particles was performed using a DSC 204F1 Phoenix (Netzsch Gerätebau GmbH, Selb, Germany). An indium standard (Tm = 156.6 °C, ΔHm = 28.5 J/g) was used to calibrate the temperature and heat flux. The measurements were performed in an argon atmosphere at a heating rate of 10 °C/min.

Production Yield

The production yield of particles was calculated based on the mass of particles obtained (W1) and the total mass of polymer and drug used (W2) by the following equation:

$$\text{Yield } (\%) = \frac{W1}{W2} \times 100$$

Estimation of Drug Loading (DL) and Drug Entrapment Efficiency (DEE)

To evaluate the entrapment efficiency (EE %) ethanol and water were added to particles and they were placed in a sonication bath to extract IDB. After filtration (PTFE, 0.45 µm, Isolab Laborgeräte Gmb, Eschau, Germany), the amount of IDB was determined by HPLC (UltiMate 3000, Thermo Scientific, Waltham, MA, USA) using an Inertsil® ODS-3HPLC column (150 × 4.6 mm, 5 µm, GL Sciences, Tokyo, Japan) under the following conditions: wavelength 281 nm, injection volume 10 µL, 1 mL/min flow rate, 25 °C oven temperature, mobile phase methanol:water in ratio 80:20.

The drug loading (DL) of the particles was calculated according to equation:

$$\text{DL } (\%) = \frac{\text{Amount of drug in the formulation (mg)}}{\text{Total amount of particles (mg)}} \times 100$$

Drug entrapment efficiency (DEE) was calculated according to the following equation:

$$\text{DEE } (\%) = \frac{\text{Actual drug content (mg)}}{\text{Theoretical drug content (mg)}} \times 100$$

In Vitro Drug Release Studies

In vitro release study was performed using the dialysis bag method. A dialysis membrane MWCO 12 kDa was cut into equal pieces (6 cm^2 × 2.5 cm^2) and hydrated in distilled water for 24 h. An accurately weighed amount of particles was dispersed in 1 mL of PBS buffer (pH 7.4), and transferred into the dialysis bag, which was closed using a plastic clamp. Each bag was placed into a beaker containing 18 mL dissolution media (PBS buffer, pH 7.4) and kept on an electromagnetic stirrer at 100 rpm and 37 ± 0.5 °C. Due to the hydrophobic nature of IDB, 1% Polysorbate 80 was added to the acceptor medium. Samples of 1 mL were withdrawn at predetermined time intervals and replaced with the equivalent volume of fresh media. The samples were filtered (PTFE, 0.45 µm, Isolab Laborgeräte Gmb, Eschau, Germany) and analyzed for drug content as described above. Mean results of triplicate measurements and standard deviation were reported.

Investigation of the Antioxidant Activity of IDB Loaded in Nanocomposite Microspheres

The ability of IDB to reduce free radicals was determined against the stable 2,2-Diphenyl-1-picryl hydrazyl (DPPH) radical [33]. DPPH is an organic, N-containing compound that dissolves in ethanol and forms solutions with a characteristic violet color and with absorption maximum at 515 nm. When a hydrogen donor (antioxidant) is added to the DPPH solution, a reduction of DPPH occurs and the color of the solution changes from violet to yellow. This change is recorded spectrophotometrically.

For the purpose of the test, 1 mg of ascorbic acid (AA), 1 mg of IDB and 12.4 mg of placebo microparticles and those loaded with drug (corresponding to 1 mg of IDB) were dispersed in 3 mL of purified water. A DPPH solution (1 mL) mixed with purified water (3 mL), which showed no antioxidant activity, was used as a control. AA is used as a

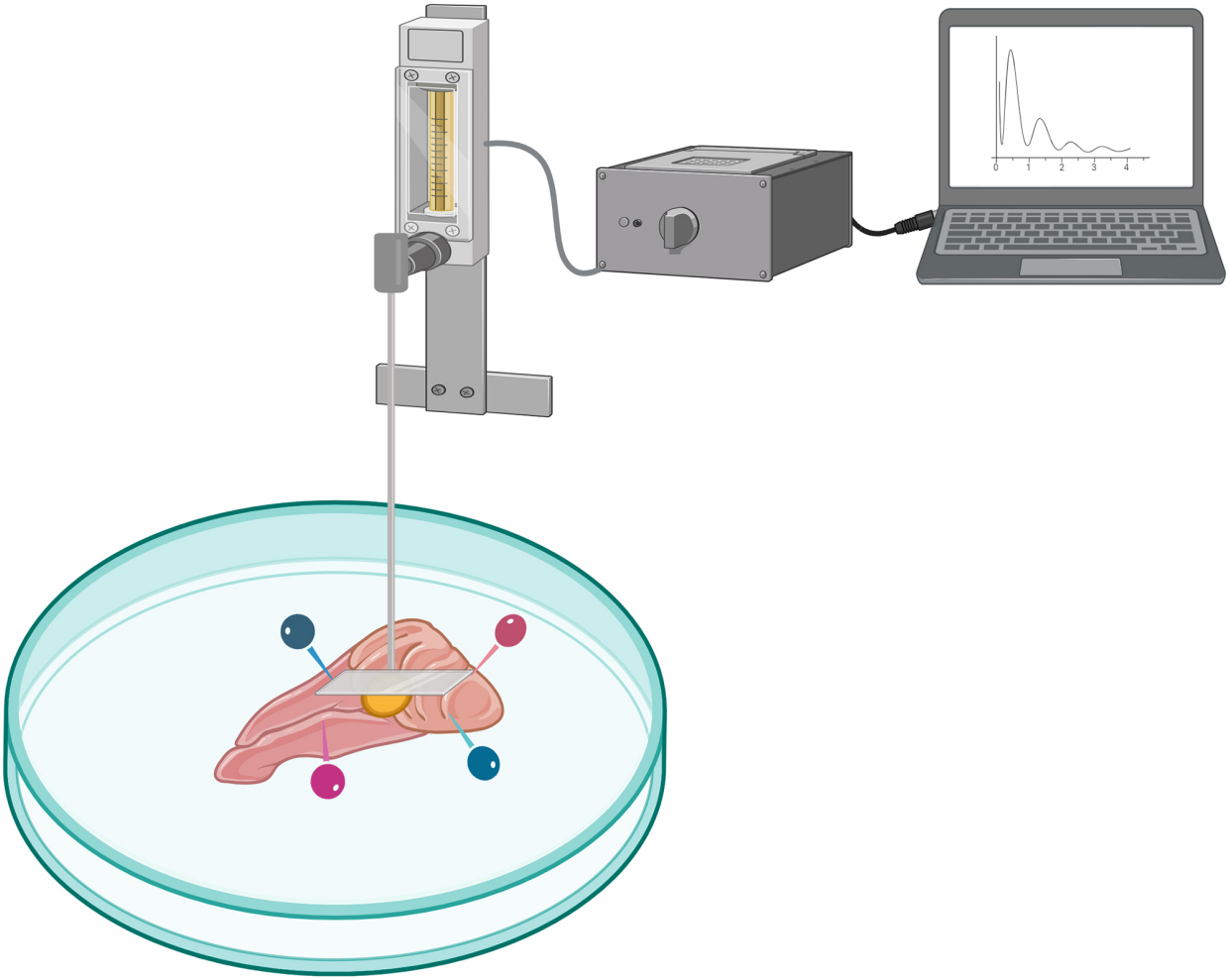

Fig. 3. Schematic representation of the experimental set-up for the study of mucoadhesive ability. Mucosa tempered at 30 °C ± 0.5 °C in contact with the surface of the nanocomposite microspheres fixed on a microscopic coverslip (created with BioRender (https://www.biorender.com)).

reference. 0.2 mM solution of DPPH in 96% ethanol was prepared and stored in the dark at 4 °C. One milliliter of the DPPH solution was added to the test dispersions. All reaction mixtures were incubated in the dark at room temperature for 1 h, then filtered (PTFE, 0.45 µm, Isolab Laborgeräte Gmb, Eschau, Germany) and absorbance was read spectrophotometrically at a wavelength of 515 nm. The results exclude interference from the excipients. The percent inhibition was calculated using the following equation:

$$\%I = \frac{A0 - A1}{A0} \times 100$$

where A0 is the absorbance of the control and A1 is the absorbance in the presence of the test substances.

Determination of the Binding Ability of IDB-Loaded Nanoparticles to Human Serum Albumin

The binding ability of the nanoparticles to human serum albumin (HSA) was investigated by fluorescence spectroscopy. Upon excitation in the range of 280 nm to 295 nm, albumin emits intensely with a major emission peak at about 340 nm [34]. To investigate a potential interaction between HSA and the model nanoparticles, the fluorescence spectra of albumin were recorded in the absence and presence of increasing amounts of the nanocomposite microspheres. In the case of interaction, the fluorescence intensity of HSA gradually decreases with increasing amount of nanoparticles [35]. Samples for analysis are prepared after dispersing a certain amount of nanocomposite microparticles in physiological solution, wherein the sodium alginate, matrix forming polymer, dissolves and releases the IDB-loaded PCL nanoparticles. After incubation with HSA solution, the potential binding of all components to albumin was assessed.

Investigation of the Mucoadhesive Ability of Nanocomposite Microstructures

The mucoadhesive ability of the nanocomposite microspheres was investigated by determining the maximum

Table 1. Preliminary experimental work to derive optimal conditions.

Conditions	Results	
Inlet temperature	Yield	Mean diameter (µm)
120 °C	No Yield	-
140 °C	Unsatisfactory Yield	<5
160 °C	Optimal Yield	>5
Gas flow rate		
400 L/h	No Yield	-
500 L/h	Unsatisfactory Yield	<5
600 L/h	Optimal Yield	>5
Speed of the peristaltic pump		
6 mL/min	Optimal Yield	>5
9 mL/min	Unsatisfactory Yield	<5
Concentration of the polymer		
0.5%	Unsatisfactory Yield	<5
1.0%	Optimal Yield	>5

Table 2. Characteristics of IDB-loaded nanocomposite microspheres (means ± SD, n = 3); drug entrapment efficiency (DEE), drug loading (DL).

Mean diameter (µm)	DEE (%)	DL (%)	Yield (%)
7.37 ± 2.4	56.68 ± 0.10	8.09 ± 0.01	66.34 ± 1.54

adhesive force applied to a unit area of freshly isolated sheep nasal mucosa [36,37]. Within one hour after the death of the animal, the nasal mucosa was dissected and fixed immobile on a paraffin disc. A cylinder was obtained by compressing 30 mg of microparticles using a hydraulic press. The cylinder was fixed in the center of a microscopic coverslip using cyanoacrylate glue and brought into contact with the mucosal surface. The value of the maximum adhesive force applied per unit area was recorded with an interface system (Fig. 3).

Statistical Analysis and Processing of Experimental Data from Mucoadhesion and Antioxidant Activity Tests

Statistical analysis was performed using GraphPad Prism 6.01 (GraphPad Software, Boston, MA, USA). To determine the statistically significant difference between the average values in the groups, a significance level of $p < 0.05$ was adopted. The data analyzed included results with statistically insignificant standard deviations from the mean, as demonstrated by Friedman's one-factor test, Friedman Analysis of Variance (ANOVA).

Results

Optimal Conditions for Obtaining Nanocomposite Microspheres (Preliminary Studies)

The spray drying was applied to obtain polymer nanocomposite microspheres. Sodium alginate was used as a polymer for the preparation of microparticles due to its proven mucoadhesive properties, biodegradation and biocompatibility [38]. Additionally, as a hydrophilic polymer, it is characterized by a high degree of swelling and optimal solubility in water, which favors the rapid release of nanoparticles incorporated in the micro-sized matrix with a view to their subsequent absorption and transport through the mechanisms of "nose-to-brain" drug delivery [25].

The conditions for obtaining nanocomposite microspheres from sodium alginate were derived as a result of preliminary experimental work (Table 1). Criteria for choosing optimal conditions are the yield and the size of the obtained microspheres.

As a result of the performed preliminary research, it was established that when the atomization is carried out at a temperature of the drying gas lower than 140 °C, the yield of microparticles is practically absent or insignificant. Drops of the polymer solution were deposited on the walls of the drying chamber. The reason for this can be found in the insufficiently high temperature for efficient evaporation of the solvent and timely solidification of the polymer and transformation of the droplets into solid particles. A similar dependence was also found in a study by Rathanand *et al.* [39]. As the inlet temperature increases, the drops sprayed through the nozzle dry faster and stick to the cylinder walls to a lesser extent. Therefore, at a higher temperature, less losses and a correspondingly higher yield are expected. In the preliminary work, the maximum yield was recorded at a drying gas temperature of 160 °C. A higher drying temperature also results in a larger particle size.

The gas flow rate was varied in the range of 400/600 L/h. At a low spraying speed (400 L/h), the material sprayed through the nozzle cannot be dried sufficiently. It is deposited on the walls of the drying chamber and this is the reason for the lack of yield of dry microparticles. Increasing the gas flow rate to 500 L/h resulted in a negligible yield of particles. Again due to significant material sticking to the walls of the spray cylinder. The highest particle yield was obtained at a gas flow rate of 600 L/h and losses during sputtering are minimized. No studies have been conducted at higher gas flow rates since a further increase in the amount of gas supplied would lead to a serious increase in the dispersity of the supplied liquid respectively to obtain particles of very small sizes. However, this is not acceptable considering the nasal route of administration of the nanocomposite microspheres and the risk of inhalation in the deep segments of the respiratory tract or removal from the nasal cavity with exhaled air. Furthermore, smaller particles are aspirated during production and lost as the end

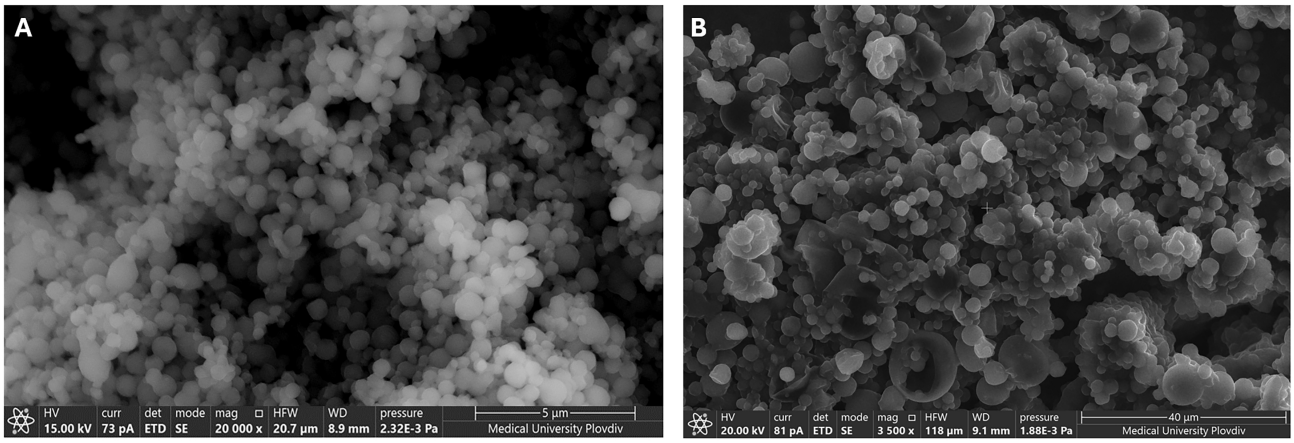

Fig. 4. SEM micrographs of IDB-loaded nanoparticles (A) (20,000×) and IDB-loaded nanocomposite microspheres (B) (3500×).

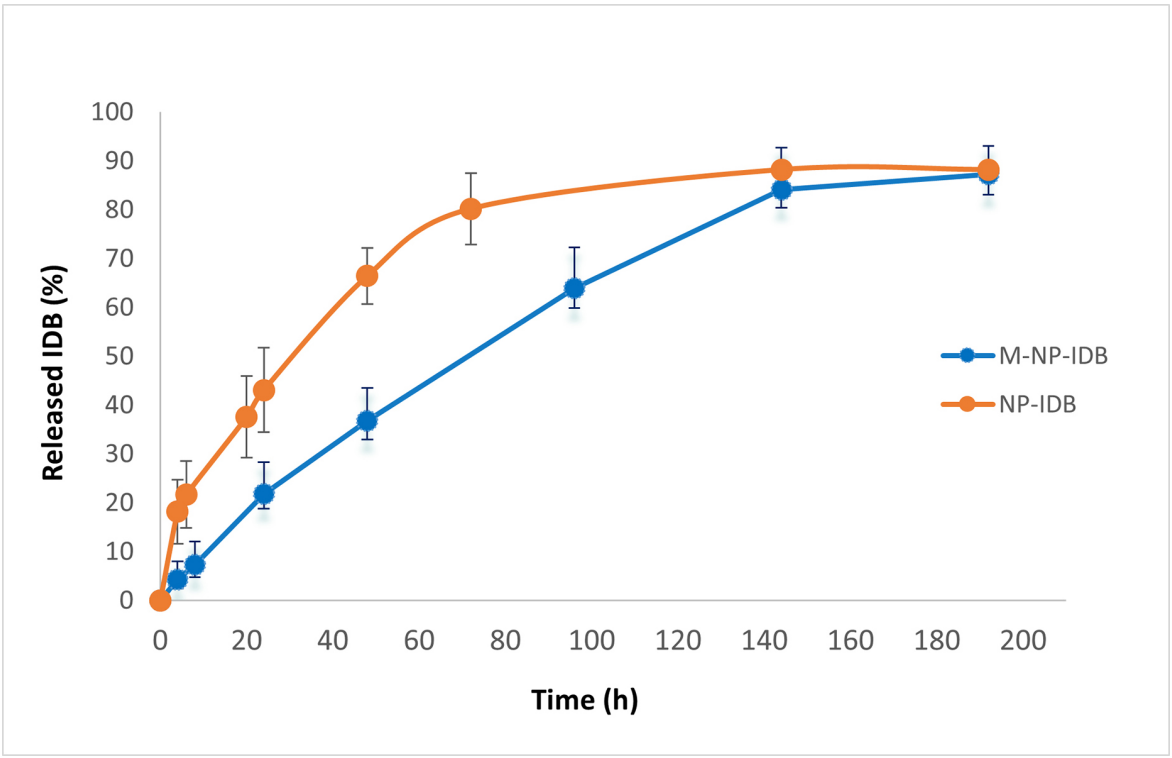

Fig. 5. Release profiles of IDB from nanoparticles and from composite microspheres.

product resulting in lower yield. Preliminary experimental work shows that a gas velocity of 600 L/h is suitable for obtaining sodium alginate nanocomposite microspheres at optimal particle yield.

Increasing the peristaltic pump speed from 6 mL/min to 9 mL/min resulted in a reduced yield. This can be explained by the fact that the faster the sample is injected, the more energy is required to evaporate the solvent from the droplets and to form dry particles. The sprayed material did not dry effectively and deposited on the walls of the spray cylinder. A peristaltic pump speed of 6 mL/min was determined to be optimal for obtaining the nanocomposite microspheres by the spray drying method. The influence of the concentration of the polymer solution on the critical parameters was also investigated. It was found that with increasing concentration from 0.5% to 1%, the average diameter of the particles increases. Based on the results of the preliminary experimental work, the following conditions for obtaining sodium alginate microspheres by the spray drying method were derived:

- Inlet temperature of the gas: 160 °C;
- Gas flow rate: 600 L/h;
- Speed of the peristaltic pump: 6 mL/min;
- Concentration of sodium alginate: 1%.

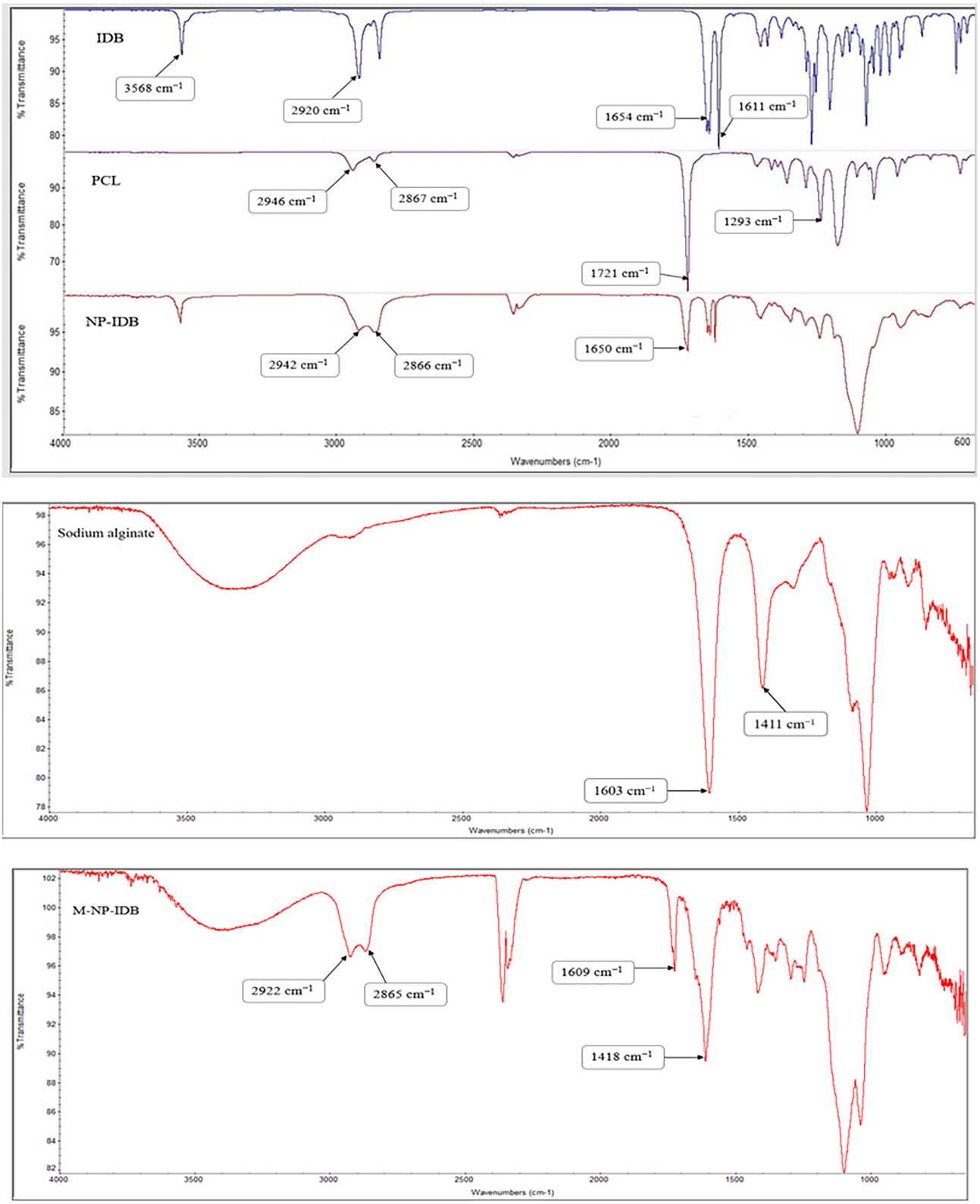

Fig. 6. Fourier-transform infrared spectroscopy (FTIR) spectra of IDB, poly-ε-caprolactone (PCL), nanoparticles loaded with IDB, sodium alginate, nanocomposite microspheres loaded with IDB (M-NP-IDB).

Characterization of Nanocomposite Microspheres

The average diameter of the obtained particles is 7.37 ± 2.4 µm (Table 2). Photomicrographs (Fig. 4) show that the obtained particles are spherical in shape and have a smooth surface, no creases or dents. High yields of about 66% were obtained.

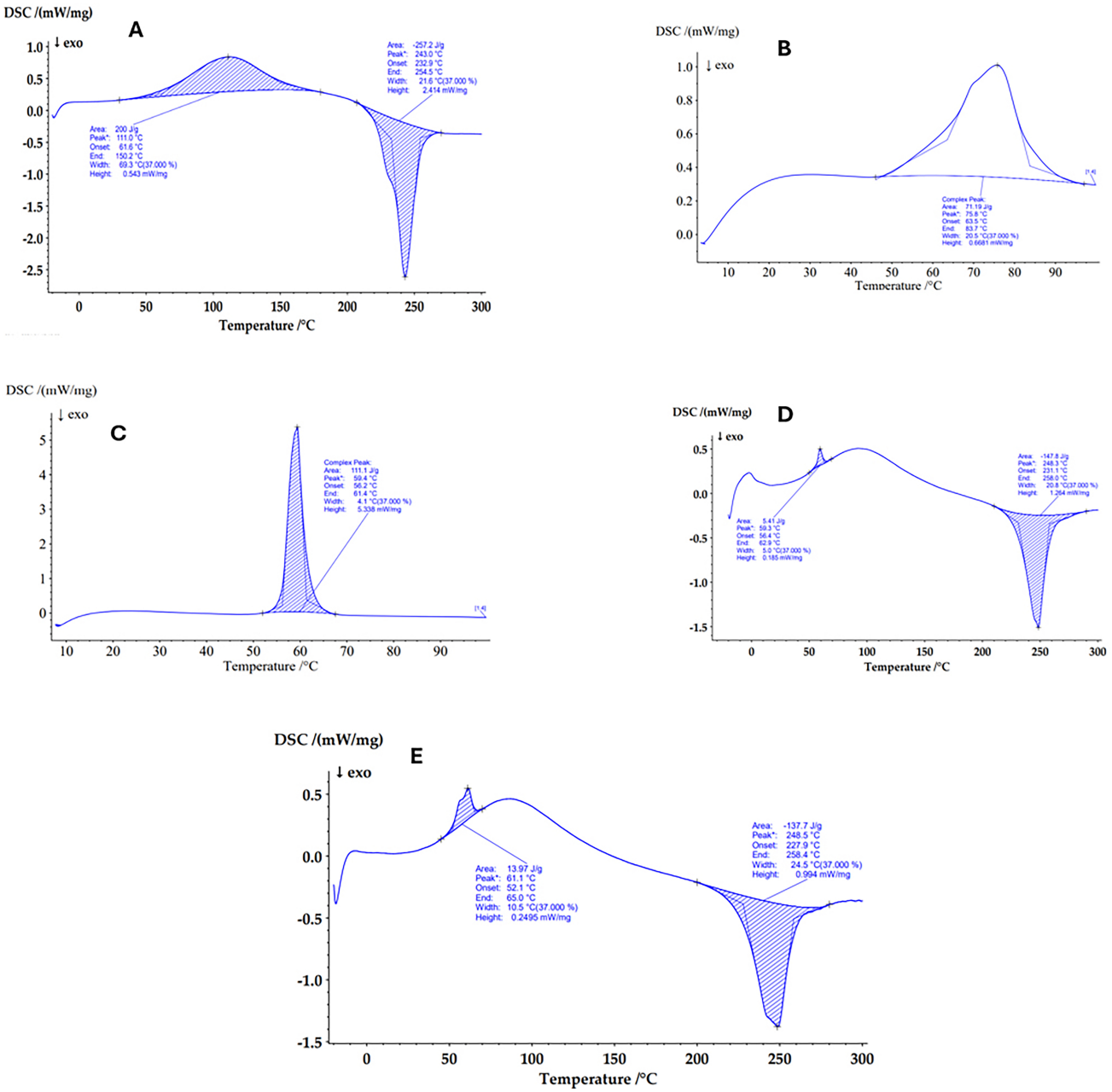

Fig. 7. DSC thermograms. Sodium alginate (A)—an endothermic peak at 111 °C corresponding to the evaporation of water molecules and an exothermic peak at 243 °C indicating oxidative polymer degradation; PCL (B)—a broad endothermic peak at about 76 °C which corresponds to the melting temperature of the polymer; IDB (C)—an endothermic peak at 60 °C corresponding to the melting point of IDB; placebo nanocomposite microspheres (D)—endothermic peak at 60 °C which is due to the PCL placebo nanoparticles included in the composite structure, second peak which is exothermic and recorded at 248 °C corresponds to the thermal decomposition of the structure-forming polymer—sodium alginate, and nanocomposite microspheres loaded with IDB (E). DSC, differential scanning calorimetry.

In Vitro Drug Release

The release of IDB from nanoparticles was prolonged finding more than 80% drug released in 72 h (Fig. 5). For comparison, inclusion of nanoparticles in a composite structure leads to an almost double delay in release—about 144 h is needed to release the same amount of IDB. The probable explanation for this is the presence of sodium alginate in the composition of microspheres which dissolves rapidly in the release medium, forms a viscous layer and thus hinders the dissolution and diffusion of the hydrophobic IDB.

FTIR Spectroscopy

The infrared spectra of IDB, PCL, sodium alginate, nanoparticles and nanocomposite microspheres loaded with IDB are shown in Fig. 6. IDB exhibits several characteristic

peaks at 3568 cm^{-1}, 2920 cm^{-1}, 2358 cm^{-1}, 1654 cm^{-1}, and 1611 cm^{-1}, corresponding to -OH, C-H, C=O groups and the C=C ring [40]. In the spectra of PCL, a doublet at 2946 cm^{-1} and 2867 cm^{-1} is observed due to symmetric and asymmetric vibrations of the aliphatic C–H bonds as well as a characteristic band for C=O at 1721 cm^{-1}. The valence vibrations of C-C and C-O bonds in the PCL molecule appear at 1293 cm^{-1}[41]. A broad characteristic peak at 3500 cm^{-1} is observed in the spectrum of sodium alginate which is due to the vibration of the large number of -OH groups in the molecule. Two characteristic peaks at 1603 cm^{-1} and 1411 cm^{-1} are distinguished due to symmetric and asymmetric vibrations of the -COO groups [42]. In the ATR spectrum of the composites, a broad characteristic band for the -OH groups of sodium alginate and IDB (3600–3000 cm^{-1}) is observed. The peak at 1418 cm^{-1} is probably due to symmetric valence vibrations of the -COO groups of alginate. The characteristic peak of PCL at 2946 cm^{-1} shifts to 2922 cm^{-1} and that at 2867 cm^{-1} shifts to 2865 cm^{-1} due to overlap with the C-H and C=O groups of IDB and alginate. The peak at 1611 cm^{-1} corresponding to the C=C ring in the IDB molecule is shifted to 1609 cm^{-1} due to overlap with the -COO groups of alginate. No new peaks are observed in the ATR spectra of the model system, which shows that during their preparation no new chemical bonds are formed as a result of interaction between the active substances and the polymers.

Differential Scanning Calorimetry (DSC)

The physical state of IDB incorporated into nanocomposite microspheres was analyzed using differential scanning calorimetry (DSC). The resulting thermograms are presented in Fig. 7. The DSC thermogram of sodium alginate shows an endothermic peak at 111 °C and an exothermic peak at 243 °C (Fig. 7A). The first peak corresponds to the evaporation of the included water molecules, while the exothermic indicate the oxidative degradation of the polymer. The thermogram of PCL demonstrated a broad endothermic peak at about 76 °C which corresponds to the melting temperature of the polymer (Fig. 7B). Similar endothermic peaks corresponding to the melting point were also observed in the IDB thermogram at 60 °C (Fig. 7C). In the DSC thermogram of the placebo nanocomposite microspheres (Fig. 7D), one endothermic peak was registered at 60 °C which is due to the PCL placebo nanoparticles included in the composite structure. The second peak which is exothermic and recorded at 248 °C corresponds to the thermal decomposition of the structure-forming polymer—sodium alginate. A single endothermic peak at 61 °C was observed in the DSC thermogram of composites loaded with IDB (Fig. 7E) which corresponds to the melting points of IDB and PCL. This is evidenced by the larger area of this peak (13.97 J/g) compared to the area of the same peak in the placebo microparticles due to the included PCL. This confirms the presence of IDB in the composite structure. The exothermic peak at 248 °C similar to the other described batch corresponds to the decomposition of alginate. No new peaks were observed in the thermograms of the nanocomposite microparticles which testifies the compatibility between the substances.

In Vitro Determination of Antioxidant Activity of IDB Incorporated into Nanocomposite Microspheres

The aim of the study was to check the antioxidant activity of IDB included in the nanocomposite microspheres compared to that of the active substance dispersed in purified water. For this purpose, a DPPH radical-reducing method was used. The method is based on electronic transfer which causes the appearance of a violet coloring which degree is established spectrophotometrically. AA is used as a reference with known high antioxidant activity. Although IDB is characterized by high reduction potential (higher than of CoQ_{10}) its activity in aqueous media is reduced due to its highly lipophilic nature [43]. The DPPH-reducing activity of IDB is 31.54% (Fig. 8) and is about three times lower than that of the reference substance.

That is probably a result of the poor solubility of IDB in aqueous media. Nanocomposite microspheres without IDB (M-NP-Placebo) also demonstrated some antioxidant capacity which is even higher than that of IDB dispersed in aqueous medium (about 40%). Possibly this activity is due to the matrix polymer—sodium alginate. Similar results were reported by Borazjani *et al.* [44] who found a dose-dependent DPPH-reducing ability of alginates as well as the possibility of reducing iron from Ferri- (Fe^{3+}) to Ferro- (Fe^{2+}) ions. The results of the present study demonstrate that incorporated IDB in the form of nanoparticles in the composite structure not only retained its antioxidant activity but also shows a significant increase result of the synergistic action of IDB and alginate.

Determination of the Binding Ability of Nanoparticles Loaded with IDB to Human Serum Albumin

Albumin is the most abundant protein in plasma and cerebrospinal fluid. It is a pliable molecule with the capability to alter its architecture depending on environmental conditions such as temperature, pH or ionic strength. It can bind many different molecules and can even act as an antioxidant [45]. Proteins such as HSA, lipoproteins, and globulin are usually adsorbed on the surface of drug-loaded nanoparticles thereby altering the *in vivo* release behavior and targeting sites of the nanoparticles [46–48].

In the present study, fluorescence spectroscopy was used for the *in situ* investigation of nanoparticle-protein interactions (Fig. 9). The analysis showed a noticeable decrease in fluorescence intensity after the addition of nanosuspension from drug-loaded nanoparticles. These results show that nanoparticles loaded with IDB interact with HSA. A fluorescence study of HSA solution with placebo

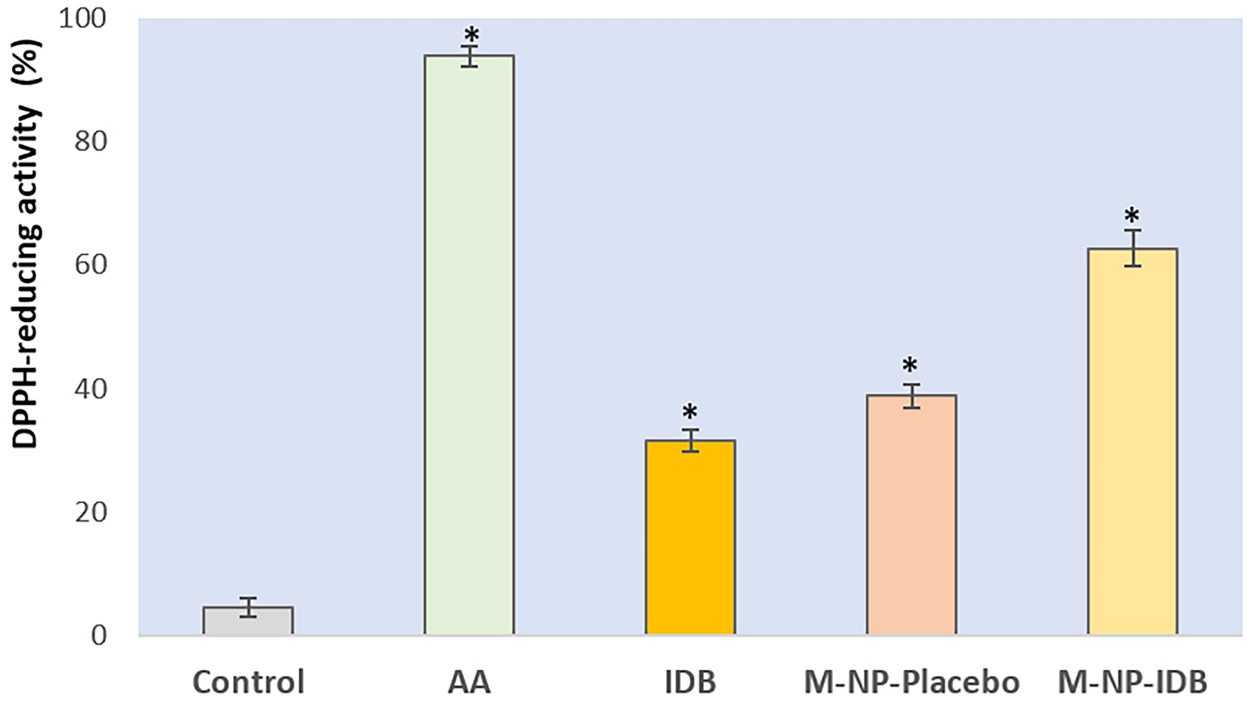

Fig. 8. 2,2-Diphenyl-1-picryl hydrazyl (DPPH)-reducing activity of ascorbic acid (AA), idebenone (IDB), nanocomposite microspheres without drug (M-NP-Placebo) and nanocomposite microspheres loaded with IDB (M-NP-IDB). Data is represented as mean values ± SD, n = 3. * indicates statistically significant result ($p < 0.05$).

nanoparticles was also performed. Negligible reduction of fluorescence emission is observed (Fig. 9) compared to that determined in drug-loaded model with increasing amount of ligand (Fig. 9). These results reveal a minor interaction of the nanosized carrier with albumin and suggest a preferential interaction of the drug substance IDB with the protein. It is logical to admit that this effect is a result of the interaction with the drug molecules. The fluorescence spectra of HSA titrated with solutions of IDB confirms that (Fig. 9). Considering, however, the low release rate of IDB from the nanocarriers (<10%, Fig. 5) within 1 h (the duration of the analysis) can be assumed that the observed decrease in fluorescence spectra is not solely due to interaction between the active substance with albumin. It can be allowed that the incorporation of drug into PCL nanoparticles significantly changes their surface properties and geometry as a result of which their affinity for binding to the protein increases dramatically.

In conclusion, it can be summarized that the loading of polymer nanoparticles with active substance is of key importance for their behavior, for possible bio-nano interactions, and hence their potential application with a view to achieving a specific therapeutic goal (targeted delivery, controlled release, etc.).

Investigation of the Mucoadhesive Ability of Nanocomposite Microstructures

In the present work, the mucoadhesive ability of nanocomposite microspheres as a drug delivery system, was investigated in direct contact with the nasal mucosa. The maximum force, required for the detach of a cylinder of pressed nanocomposite microparticles from native sheep nasal mucosa after different time contact (1, 3, 5, 10, 15, and 25 min) is determined. The results of the study (Fig. 10) show a high degree of attachment to the nasal mucosa.

The chronological change in adhesion strength showed a statistically significant difference at all time points compared to the initial moment which is an indicator of achieving a high degree of attachment even after one minute of contact with the nasal mucosa. As the contact time increases, the maximum adhesive strength increases and reaches a maximum after five minutes of contact. It was established that a contact time longer than 5 min does not lead to an additional increase in adhesive strength, and even vice versa, a decrease and reaching a stable mechanical tension is recorded after 15 min. There is no statistical difference between placebo nanocomposite microspheres and those loaded with IDB in terms of their adhesive properties. These results highlight the adhesive ability of the developed composite structure and are a guarantee for their reliable delivery in the nasal cavity.

Discussion

As previously reported the emulsion/solvent evaporation technique allows the preparation of PCL nanoparticles with suitable structural and morphological characteristics for nose-to-brain delivery of IDB [32]. Although after nasal

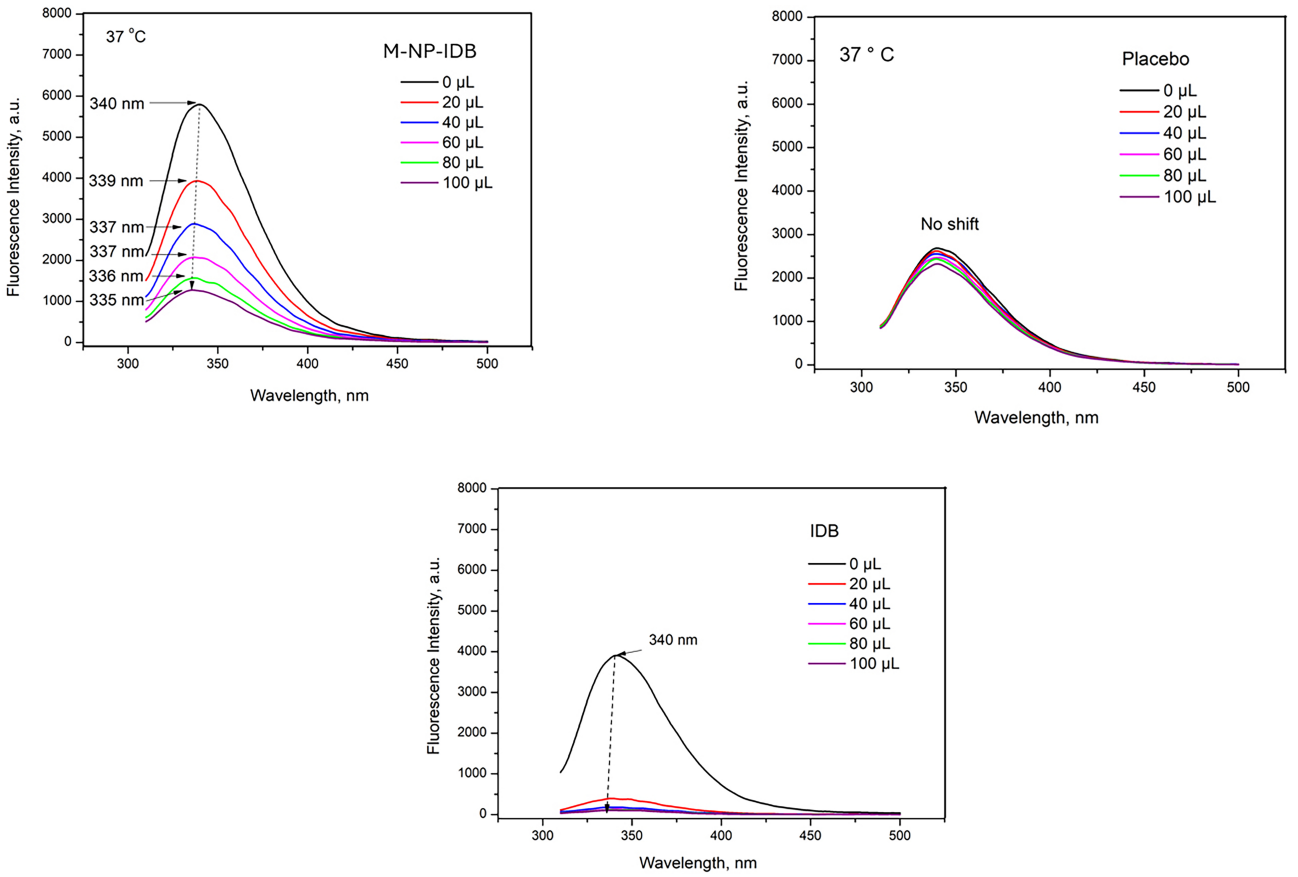

Fig. 9. Fluorescence spectra of human serum albumin (HSA) (2.7 mg/mL) upon addition of different volumes of samples containing dispersed drug-loaded particles (M-NP-IDB), placebo particles (Placebo), and upon titration with IDB.

administration due to their small size, nanoparticles follow the respiratory tract and leave the nasal cavity without being deposited in it. It is necessary to incorporate the nanostructures developed so far into a carrier, which on the one hand has optimal dimensions for preferential deposition in the nasal cavity (about 5 µm), and on the other hand it is characterized by sufficiently good adhesive ability, which will create conditions for prolonged contact with the nasal mucosa and the possibility of penetration through it. Optimizing the carrier size in the micro-range is a potential strategy for the deposition of drug-loaded particles in the olfactory region.

Nanocomposite microspheres of sodium alginate containing the drug-loaded nanoparticles were successfully obtained by spray drying. It is a widely utilized technique for producing polymer microparticles due to its simplicity, scalability, and versatility. Study the influence of the technological parameters of the spray drying process is of decisive importance for the qualities of the obtained product. The dependencies derived in the literature serve only as a guide, as there are no universal models for determining the optimal drying conditions for each specific case. It allows for the adjustment of process parameters to achieve particles with desired characteristics, making it an attractive method for both research and industrial applications. However, one common disadvantage of spray drying, as with many microparticle preparation methods, is the poor uniformity of the resulting particles. Spray drying involves atomizing a liquid solution into a hot drying chamber, where rapid solvent evaporation occurs, forming solid particles. Variations in droplet size during atomization lead to differences in drying rates and ultimately in particle size and shape. This inherent variability in the process contributes to the lack of uniformity. When formulating composite microparticles, especially those loaded with nanostructures, achieving uniformity becomes even more challenging. The incorporation of nanostructures can lead to heterogeneous distribution within the particles, further contributing to size and shape variations. Small particles, particularly those on the micro- and nano-scale, are prone to aggregation due to high surface energy and attractive inter-particle forces. Aggregation can lead to the formation of larger, irregularly shaped particles, further reducing uniformity. Despite these challenges, spray drying remains a preferred method for producing microparticles due to its ability to scale up and adjust parameters to meet specific needs. By optimizing parameters such as feed rate, atomization pressure, and drying temperature, it is possible to achieve particles within a targeted size range, which is crucial for applications requiring specific administration routes. Our goal was to pro-

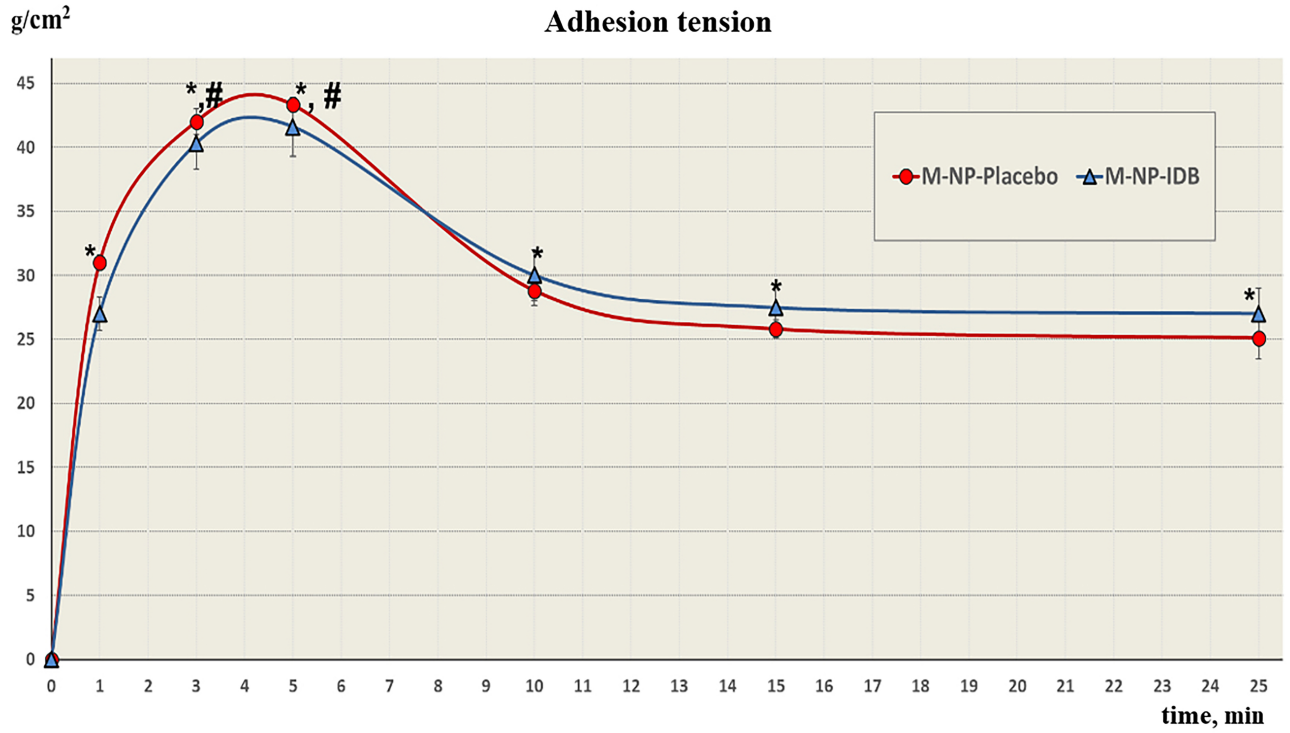

Fig. 10. Chronological change of maximal adhesion force of placebo microcomposites (M-NP-Placebo) and microcomposites loaded with IDB (M-NP-IDB). The symbols * and # indicate the presence of a reliable statistical difference compared to the initial moment (*), and after the established steady state of the process 15 min (#).

duce microparticles with an average diameter suitable for the intended administration route. The resulting particles achieved this average diameter, though naturally included both smaller and larger particles. This size distribution and the observed variations in particle size and shape are typical and expected in spray drying processes, especially in formulations involving composite microparticles loaded with nanostructures. Despite these challenges, the method allows the production of microparticles within a desired size range, meeting our primary goals for the intended application.

Evaluation of mucoadhesive properties is essential for the design of drug delivery systems for nasal administration. Overcoming mucociliary clearance, is a prerequisite for prolonged contact between the administered dosage form and the nasal mucosa, and hence for the higher degree of penetration through the nasal epithelium. The great interest in mucoadhesive microspheres and their wide application as drug delivery systems is due to their numerous advantages. As a result of better contact and adhesion, the system remains for a long time at the applied site and thus creates an opportunity to increase the bioavailability of the active substance at a reduced concentration. The increased residence time combined with controlled release of drug is a prerequisite for reducing frequency of administartion, which ensures patient convenience and increased compliance. The use of polymers with good adhesion properties makes it possible to direct the action to specific target tissues or organs, and the use of alternative routes of administartion such as nasal makes it possible to achieve high bioavailability of drugs with pronounced “first-pass” metabolism. There is an opportunity to control the release behavior of the active substance and the degradation of the particles by the choice of components to build the matrix. The composites we developed demonstrated a high degree of attachment to sheep nasal mucosa, suggesting a gradual release of the drug-loaded nanoparticles, which could subsequently move to the CNS by intra- and paracellular transport mechanisms via the olfactory region and trigeminal nerve.

However, apart from the performed general physicochemical characterisation and proved mucoadhesive properties of composites, further studies are ongoing to demonstrate, both behaviorally and biochemically IDB’s activity.

Conclusions

IDB-loaded PCL nanoparticles were successfully incorporated into composite microspheres by spray drying. The composite structures have dimensions ranging of 7.37 $\pm$ 2.4 µm and high mucoadhesive ability which makes them suitable for nasal administration. The inclusion of IDB in PCL nanoparticles and the subsequent incorporation of nanoparticles into composite microspheres do not lead to a change in biological properties (antioxidant activity of

idebenone). There are no chemical interactions between medicinal substances and polymers, which is reason to accept that they are compatible. The binding affinity of PCL nanoparticles to human serum albumin was determined by their loading with drug.

Abbreviations

AA, ascorbic acid; AD, Alzheimer's disease; CNS, central nervous system; DPPH, 2,2-Diphenyl-1-picryl hydrazyl; HSA, human serum albumin; IDB, idebenone; N2B, nose-to-brain; PCL, poly-ε-caprolactone.

Availability of Data and Materials

All data generated or analyzed during this study are included in this published article.

Author Contributions

RB and BP designed the research study. RB, PK, AH, SA and PZ performed the research. PZ provided help and advice on mucoadhesion study and analyzed the data. RB and BP wrote the manuscript. All authors contributed significantly to editorial changes of important content. All authors read and approved the final manuscript. All authors have participated sufficiently in the work and agreed to be accountable for all aspects of the work.

Ethics Approval and Consent to Participate

Not applicable.

Acknowledgment

Not applicable.

Funding

This research received funding from Medical University of Plovdiv, project № HO-15/2023.

Conflict of Interest

The authors declare no conflict of interest.

References

[1] Silva MVF, Loures CDMG, Alves LCV, de Souza LC, Borges KBG, Carvalho MDG. Alzheimer's disease: risk factors and potentially protective measures. Journal of Biomedical Science. 2019; 26: 33.

[2] Hebert LE, Weuve J, Scherr PA, Evans DA. Alzheimer disease in the United States (2010-2050) estimated using the 2010 census. Neurology. 2013; 80: 1778–1783.

[3] Salim S. Oxidative Stress and the Central Nervous System. The Journal of Pharmacology and Experimental Therapeutics. 2017; 360: 201–205.

[4] Cobley JN, Fiorello ML, Bailey DM. 13 reasons why the brain is susceptible to oxidative stress. Redox Biology. 2018; 15: 490–503.

[5] Uttara B, Singh AV, Zamboni P, Mahajan RT. Oxidative stress and neurodegenerative diseases: a review of upstream and downstream antioxidant therapeutic options. Current Neuropharmacology. 2009; 7: 65–74.

[6] Passeri E, Elkhoury K, Morsink M, Broersen K, Linder M, Tamayol A, *et al*. Alzheimer's Disease: Treatment Strategies and Their Limitations. International Journal of Molecular Sciences. 2022; 23: 13954.

[7] Feng Y, Wang X. Antioxidant therapies for Alzheimer's disease. Oxidative Medicine and Cellular Longevity. 2012; 2012: 472932.

[8] Fadda LM, Hagar H, Mohamed AM, Ali HM. Quercetin and Idebenone Ameliorate Oxidative Stress, Inflammation, DNA damage, and Apoptosis Induced by Titanium Dioxide Nanoparticles in Rat Liver. Dose-Response. 2018; 16: 1559325818812188.

[9] Jiang W, Geng H, Lv X, Ma J, Liu F, Lin P, *et al*. Idebenone Protects against Atherosclerosis in Apolipoprotein E-Deficient Mice Via Activation of the SIRT3-SOD2-mtROS Pathway. Cardiovascular Drugs and Therapy. 2021; 35: 1129–1145.

[10] Gueven N, Ravishankar P, Eri R, Rybalka E. Idebenone: When an antioxidant is not an antioxidant. Redox Biology. 2021; 38: 101812.

[11] Thal LJ, Grundman M, Berg J, Ernstrom K, Margolin R, Pfeiffer E, *et al*. Idebenone treatment fails to slow cognitive decline in Alzheimer's disease. Neurology. 2003; 61: 1498–1502.

[12] Schlatter J, Bourguignon E, Majoul E, Kabiche S, Balde IB, Cisternino S, *et al*. Stability study of oral pediatric idebenone suspensions. Pharmaceutical Development and Technology. 2017; 22: 296–299.

[13] Kadry H, Noorani B, Cucullo L. A blood-brain barrier overview on structure, function, impairment, and biomarkers of integrity. Fluids and Barriers of the CNS. 2020; 17: 69.

[14] Achar A, Myers R, Ghosh C. Drug Delivery Challenges in Brain Disorders across the Blood-Brain Barrier: Novel Methods and Future Considerations for Improved Therapy. Biomedicines. 2021; 9: 1834.

[15] Pardridge WM. Drug transport across the blood-brain barrier. Journal of Cerebral Blood Flow and Metabolism. 2012; 32: 1959–1972.

[16] Belur LR, Romero M, Lee J, Podetz-Pedersen KM, Nan Z, Riedl MS, *et al*. Comparative Effectiveness of Intracerebroventricular, Intrathecal, and Intranasal Routes of AAV9 Vector Administration for Genetic Therapy of Neurologic Disease in Murine Mucopolysaccharidosis Type I. Frontiers in Molecular Neuroscience. 2021; 14: 618360.

[17] Jeong SH, Jang JH, Lee YB. Drug delivery to the brain via the nasal route of administration: exploration of key targets and major consideration factors. Journal of Pharmaceutical Investigation. 2023; 53: 119–152.

[18] Wang Z, Xiong G, Tsang WC, Schätzlein AG, Uchegbu IF. Nose-to-Brain Delivery. The Journal of Pharmacology and Experimental Therapeutics. 2019; 370: 593–601.

[19] Govender M, Indermun S, Kumar P, Choonara YE. Potential Targeting Sites to the Brain Through Nasal Passage. In Pathak YV, Yadav HKS (eds.) Nasal Drug Delivery. Springer: Cham. 2023.

[20] Frey WH III. Neurologic agents for nasal administration to the brain. 1991. Available at: https://patentscope.wipo.int/search/en/detail.jsf?docId=WO1991007947&tab=PCTBIBLIO (Accessed: 1 March 2024).

[21] Lochhead JJ, Thorne RG. Intranasal delivery of biologics to the central nervous system. Advanced Drug Delivery Reviews. 2012; 64: 614–628.

[22] Dahlin M, Jansson B, Björk E. Levels of dopamine in blood and brain following nasal administration to rats. European Journal of Pharmaceutical Sciences. 2001; 14: 75–80.
[23] Born J, Lange T, Kern W, McGregor GP, Bickel U, Fehm HL. Sniffing neuropeptides: a transnasal approach to the human brain. Nature Neuroscience. 2002; 5: 514–516.
[24] Craft S, Baker LD, Montine TJ, Minoshima S, Watson GS, Claxton A, *et al*. Intranasal insulin therapy for Alzheimer disease and amnestic mild cognitive impairment: a pilot clinical trial. Archives of Neurology. 2012; 69: 29–38.
[25] Gänger S, Schindowski K. Tailoring Formulations for Intranasal Nose-to-Brain Delivery: A Review on Architecture, Physico-Chemical Characteristics and Mucociliary Clearance of the Nasal Olfactory Mucosa. Pharmaceutics. 2018; 10: 116.
[26] Fortuna A, Alves G, Serralheiro A, Sousa J, Falcão A. Intranasal delivery of systemic-acting drugs: small-molecules and biomacromolecules. European Journal of Pharmaceutics and Biopharmaceutics. 2014; 88: 8–27.
[27] Lengyel M, Kállai-Szabó N, Antal V, Laki AJ, Antal I. Microparticles, Microspheres, and Microcapsules for Advanced Drug Delivery. Scientia Pharmaceutica. 2019; 87: 20.
[28] Yarragudi SB, Richter R, Lee H, Walker GF, Clarkson AN, Kumar H, *et al*. Formulation of olfactory-targeted microparticles with tamarind seed polysaccharide to improve nose-to-brain transport of drugs. Carbohydrate Polymers. 2017; 163: 216–226.
[29] Yarragudi SB, Kumar H, Jain R, Tawhai M, Rizwan S. Olfactory Targeting of Microparticles Through Inhalation and Bi-directional Airflow: Effect of Particle Size and Nasal Anatomy. Journal of Aerosol Medicine and Pulmonary Drug Delivery. 2020; 33: 258–270.
[30] Omanović-Mikličanin E, Badnjević A, Kazlagić A, Hajlovac M. Nanocomposites: A brief review. Health and Technology. 2020; 10: 51–59.
[31] Nicolai L, Gloria A, Ambrosio L. The mechanics of biocomposites. In Ambrosio L (ed.) Biomedical Composites (pp. 411–440). 1st edn. CRC Press: London, UK. 2010.
[32] Boyuklieva R, Hristozova A, Pilicheva B. Synthesis and Characterization of PCL-Idebenone Nanoparticles for Potential Nose-to-Brain Delivery. Biomedicines. 2023; 11: 1491.
[33] Yang H, Yu S, Kim J, Baek K, Lee YR, Lee HS, *et al*. Facile Solvent-Free Preparation of Antioxidant Idebenone-Loaded Nanoparticles for Efficient Wound Healing. Pharmaceutics. 2022; 14: 521.
[34] Peters T. The Albumin Molecule: Its Structure and Chemical Properties. In Peters T (ed.) All about Albumin: Biochemistry, Genetics and Medical Applications (pp. 9–75). 1st edn. Academic Press: San Diego. 1995.
[35] Ray A, Seth BK, Pal U, Basu S. Nickel(II)-Schiff base complex recognizing domain II of bovine and human serum albumin: spectroscopic and docking studies. Spectrochimica Acta. Part A, Molecular and Biomolecular Spectroscopy. 2012; 92: 164–174.
[36] Davidovich-Pinhas M, Harari O, Bianco-Peled H. Evaluating the mucoadhesive properties of drug delivery systems based on hydrated thiolated alginate. Journal of Controlled Release. 2009; 136: 38–44.
[37] Tangri P, Khurana S, Satheesh M. Mucoadhesive drug delivery: mechanism and method of evaluation. International Journal of Pharma and Bio Sciences. 2011; 2: 458–467.
[38] Frent OD, Vicas LG, Duteanu N, Morgovan CM, Jurca T, Pallag A, *et al*. Sodium Alginate-Natural Microencapsulation Material of Polymeric Microparticles. International Journal of Molecular Sciences. 2022; 23: 12108.
[39] Rathananand M, Kumar D, Shirwaikar A, Kumar R, Sampath Kumar D, Prasad R. Preparation of mucoadhesive microspheres for nasal delivery by spray drying. Indian Journal of Pharmaceutical Sciences. 2007; 69: 651.
[40] Varela-Fernández R, Lema-Gesto MI, González-Barcia M, Otero-Espinar FJ. Design, development, and characterization of an idebenone-loaded poly-ε-caprolactone intravitreal implant as a new therapeutic approach for LHON treatment. European Journal of Pharmaceutics and Biopharmaceutics. 2021; 168: 195–207.
[41] Badri W, Miladi K, Robin S, Viennet C, Nazari QA, Agusti G, *et al*. Polycaprolactone Based Nanoparticles Loaded with Indomethacin for Anti-Inflammatory Therapy: From Preparation to Ex Vivo Study. Pharmaceutical Research. 2017; 34: 1773–1783.
[42] Badita CR, Aranghel D, Burducea C, Mereuta P. Characterization of sodium alginate based films. Romanian Journal of Physics. 2020; 65: 1–8.
[43] Pignatello R, Acquaviva R, Campisi A, Raciti G, Musumeci T, Puglisi G. Effects of liposomal encapsulation on the antioxidant activity of lipophilic prodrugs of idebenone. Journal of Liposome Research. 2011; 21: 46–54.
[44] Borazjani NJ, Tabarsa M, You S, Rezaei M. Effects of extraction methods on molecular characteristics, antioxidant properties and immunomodulation of alginates from Sargassum angustifolium. International Journal of Biological Macromolecules. 2017; 101: 703–711.
[45] Picón-Pagès P, Bonet J, García-García J, Garcia-Buendia J, Gutierrez D, Valle J, *et al*. Human Albumin Impairs Amyloid β-peptide Fibrillation Through its C-terminus: From docking Modeling to Protection Against Neurotoxicity in Alzheimer's disease. Computational and Structural Biotechnology Journal. 2019; 17: 963–971.
[46] Yuan L, Cao Y, Luo Q, Yang W, Wu X, Yang X, *et al*. Pullulan-Based Nanoparticle-HSA Complex Formation and Drug Release Influenced by Surface Charge. Nanoscale Research Letters. 2018; 13: 317.
[47] Dai J, Chen C, Yin M, Li H, Li W, Zhang Z, *et al*. Interactions between gold nanoparticles with different morphologies and human serum albumin. Frontiers in Chemistry. 2023; 11: 1273388.
[48] Maffre P, Brandholt S, Nienhaus K, Shang L, Parak WJ, Nienhaus GU. Effects of surface functionalization on the adsorption of human serum albumin onto nanoparticles - a fluorescence correlation spectroscopy study. Beilstein Journal of Nanotechnology. 2014; 5: 2036–2047.